

APSE-NET: DEEP LEARNING BASED APPLE LEAF DISEASE DETECTION VIA DEGONET AND GSACMNET

Sarika Tanajirao Thorat ^{1,*}, and Rahul Kumar Budania ²

¹ Research Scholar, Department of Electronics & Communication Engineering, Shri Jagdishprasad Jhabarmal Tibrewala University, Vidyanagari, Jhunjhunu, Rajasthan, India

² Assistant Professor, & Head of Department, Electronics & Communication Engineering, Shri Jagdishprasad Jhabarmal Tibrewala University, Vidyanagari, Jhunjhunu, Rajasthan, India

*Corresponding e-mail: sarikapatil1211@gmail.com

Abstract – Apple leaf diseases (APD) significantly impact tree health and crop yield by causing leaf damage, reducing photosynthesis, and making trees more susceptible to other infections. However, existing techniques struggle with detecting multiple diseases, lighting variations, and generalizing across different cultivation conditions. To overcome this challenge, a novel deep learning-based APSE-NET is proposed for APD detection. The input images are collected from Turkey Plant Dataset and preprocessed by Joint Bilateral Filter (JBF) to reduce the noise and enhance the image quality. The denoised images are fed into DenseGoogleNet (DeGoNet) that combines the dense connectivity of DenseNet with the architectural principles of GoogleNet (Inception modules) to efficiently capture multi-scale features. Gated Self-Attentive Convolved MobileNetV3 (GSACMNet) is a lightweight deep learning model that integrates self-attention and gating mechanisms into MobileNetV3, enabling it to focus on important regions of the image. It effectively uses the extracted features for accurate and efficient classification. The proposed APSE-NET model is assessed based on its f1 score (F1), specificity (SP), precision (PR), recall (RE) and accuracy (AC). The proposed APSE-NET model achieves a high accuracy of 98.89% in ALD classification. Compared to CBAM, DWT and CNN the proposed model improves overall accuracy by 4.88%, 0.26% and 2.74% respectively.

Keywords – Apple leaf diseases, Turkey Plant Dataset, Joint Bilateral Filter, DenseGoogleNet, Gated Self-Attentive Convolved MobileNetV3.

1. INTRODUCTION

One of the most popular fruits in the world, apples are grown all over the world [1]. Because of its excellent nutritional and therapeutic qualities, apples are among the most prolific fruits [2]. More than seventy-five percent of all apples produced in India are produced in the Valley of Kashmir [3]. According to the Directorate of Horticulture (2021), apples are currently grown on around 160000 hectares of land in the Valley, with an annual production of about 180000 MTs, of which a significant amount is exported to other countries [4]. However, each year, illnesses and pests cost the apple sector a significant amount of money. Apple

farmers continue to face a serious danger from diseases including Alternaria, Scab, and Mosaic [5].

Seasons and other variables like temperature, humidity, CO2 concentration, and water availability all affect the patterns of plant diseases [6]. Since each illness may react differently to these changes, these variables can have a remarkable impact on the progression of the disease [7]. Additionally, different lighting conditions can sometimes make the visual symptoms of different diseases appear similar. However, other factors, such as leaf morphology, nonhomogeneous background, age of infected cells, variations in leaf color, and light illumination during imaging, can cause disease patterns to differ significantly [8,9]. In this study, DL-based APSE-NET model has been proposed for APD detection. The key contributions of this work are summarized as,

- The apple leaf images are preprocessed using a JBF, which enhances image quality by simultaneously preserving edge structures and reducing noise, ensuring that fine details and texture important for APD are retained.
- The denoised images are fed into DeGoNet that combines the dense connectivity of DenseNet with the architectural principles of GoogleNet (Inception modules) to efficiently capture multi-scale features.
- GSACMNet integrates self-attention and gating mechanisms into MobileNetV3, enabling it to focus on significant regions of the image. It effectively uses the extracted features for accurate and efficient classification.
- The efficacy of the proposed APSE-NET was evaluated using the specific metrics like AC, F1, SP, PR and RE.

The structure of the paper is organized as follows, section-2 describes the literature survey, the APSE-NET was explained in section-3, the performance outcomes and their

comparison analysis were provided in section-4 and section-5 comprises with conclusion and future work

2. LITERATURE SURVEY

In recent years, several researches have investigated for the APD detection with DL and ML methods. The section that follows provides a review of some current research papers.

In 2022, Wang, Y., et al., [10] proposed the use of a Ghost Attention YOLO network (MGA-YOLO) to diagnose ALD in real time on mobile devices. The Convolutional Block Attention Module (CBAM) and Mobile Inverted Residual Bottleneck Convolution were added to improve the YOLO network's feature extraction capabilities. Additionally, after applying image augmentation techniques to the dataset, our method's mAP to 94.0%.

In 2022, Hasan, S., et al., [11] proposed three components: categorization, feature extraction, and sick area segmentation. Images of Apple Scab, Black Rot, and Cedar Apple Rust illness are used in this paper's experiment on the dataset to train and test our model. With an accuracy of 98.63%, the combination of suggested DWT and color histogram characteristics offers a unique method for identifying and diagnosing apple leaf disease.

In 2023, Gong, X. and Zhang, S., [12] proposed the Faster R-CNN technique for APD. For the purpose of extracting dependable and multi-dimensional features, the sophisticated Res2Net and feature pyramid network architectures were presented as feature extraction networks. The improved Faster R-CNN structure performs better than previous item recognition methods in the annotated APD dataset, with an average precision of 63.1%.

In 2022, Di, J. and Li, Q., [13] proposed an enhanced convolutional neural network-based technique for identifying ALD. According to the findings, the DFTiny-YOLO model's mean average precision (mAP) and average IoU were 99.99% and 90.88%, respectively, and its detection speed was 280 frames per second. The performance is much

enhanced by the novel approach put forward in this study when compared to the Tiny-YOLO and YOLOv2.

In 2021 Bansal, P., et al., [14] proposed a DL method to categorize apple tree diseases. On the validation dataset, the accuracy of our suggested model is 96.25%. The suggested model can identify leaves with multiple diseases by 90% accuracy. The suggested model performed well on a variety of measures and may be used in the agriculture industry to quickly and precisely determine the health of plants.

In 2025 Huang, X., [15] proposed a classification model for APD that combines ConvNeXt and Transformer. When evaluated on a separate dataset, the suggested EConv-ViT model produced accuracy rates of 79.3% on photographs taken in natural settings and 99.2% on images taken in a lab. On a dataset taken in real settings, the EConv-ViT model's classification accuracy improved by 18.6%, 36.1%, and 37.8% when compared to the ViT, ConvNeXt, and ResNet50 models.

In 2025 Bao, W. and Zhang, F., [16] proposed an apple pest and disease detection network that uses effective hierarchical feature fusion and partial multi-scale feature extraction. By adding a wide kernel attention mechanism, LKAP broadens the receptive field and improves the accuracy of diseased area localization. Experimental findings show that YOLO-PEL achieves a mAP@50 of 72.9% in the Turkey_Plant dataset apple subset, outperforming the baseline YOLOv11 by around 4.3%.

However, existing techniques struggle with detecting multiple diseases, lighting variations, and generalizing across different cultivation conditions. To overcome this challenge, a novel deep learning-based APSE-NET is proposed for ALD detection

3. PROPOSED METHODOLOGY

In this research, a novel DL-based APSE-NET model is proposed for APD detection. Figure 1 displays the APSE-NET methodology.

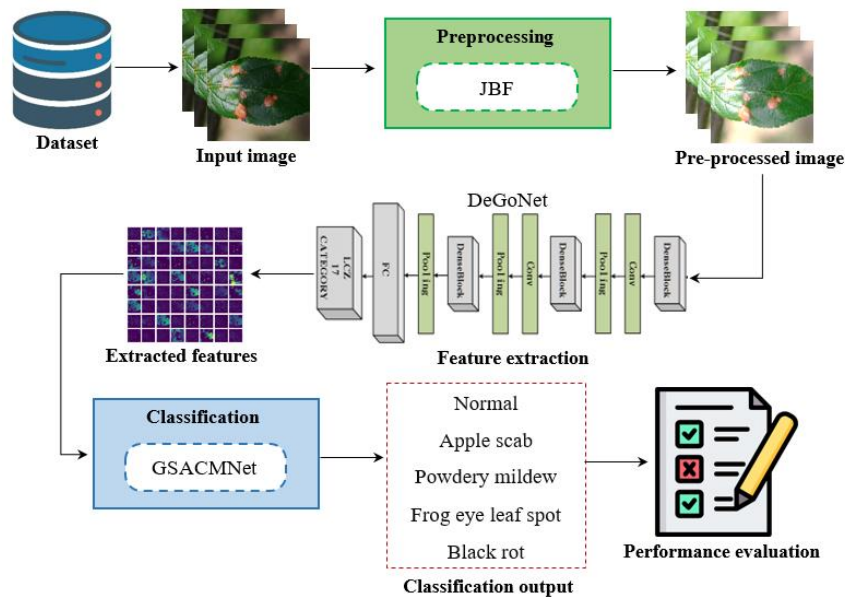


Figure 1. Proposed APSE-NET methodology

3.1 Dataset description

The Turkey_Plant Dataset, an open-source dataset created for plant disease and pest detection research, contains the apple pest and disease subset that is used in this work. The dataset consists of 4000×6000 pixel three-channel (RGB) color photos taken using a Nikon 7200d camera. It also has unrestricted photos of a variety of landscapes, including dirt, trees, leaves, and the sky. It addresses a number of prevalent pest and disease issues that arise throughout the apple-growing process, including apple scab disease and apple woolly aphid infestation. The original dataset consists of 1416 high-resolution photos of diseases and pests of apple leaves that were taken at various times, in various locations, and in various lighting situations.

3.2 Preprocessing

The JBF is a popular nonlinear edge-preserving filter that was used extensively in image fusion lately because of how well it stabilizes BF weights and avoids partial reversals close to edges. JBF is a bilateral filtering-based image filtering method that efficiently eliminates noise while maintaining image details by processing color and spatial information at the same time.

$$I_{JBF}(i) = \frac{1}{K(i)} \sum_{i \in S} e^{-\frac{\|i-j\|^2}{\sigma_s^2}} e^{-\frac{\|G(i)-G(j)\|^2}{\sigma_r^2}} \quad (1)$$

where the spatial coordinates are i and j , the normalization factor is $K(i)$, the guiding image is G , the spatial filtering intensity is σ_s , the intensity filtering asset is σ_r , and the JBF's output is $I_{JBF}(i)$.

The filtering process is guided and constrained by the guidance image G , which improves the preservation of texture features and edges. The filtering algorithm is capable of more accurate filtering operations by using information from the guide image to better understand the image's structure. The general formula for the image's JBF decomposition is as follows:

$$F_{JBF} = JBF(I, G, \sigma_s, \sigma_r) \quad (2)$$

3.3 Feature extraction

In this section the denoised images are processed using DenseGoogleNet (DeGoNet) for feature extraction. It is a combination of DenseNet with an inception model from GoogLeNet. It uses a hierarchical feature extraction approach in conjunction with effective feature reuse to extract relevant characteristics from images. A cutting-edge CNN architecture for visual object detection with fewer parameters is called DenseNet. With a few key differences, DenseNet and ResNet are fairly comparable. The output layers (i^{th}) are often calculated using conventional CNNs applying the output of the previous layer Y_{i-1} to a non-linear transformation $R_i(\cdot)$.

$$Y_i = R_i(Y_{i-1}) \quad (3)$$

DenseNet concatenates the layer output functionality maps with the inputs rather than summarizing them separately. To enhance information flow across layers, A straightforward model is offered by DenseNet: The features

of the previous layers' inputs are transmitted to the i^{th} layer. The equation (6) is then changed to:

$$Y_i = R_i([Y_0, Y_1, Y_2, \dots, Y_{i-1}]) \quad (4)$$

where $[Y_0, Y_1, Y_2, \dots, Y_{i-1}]$ is a single tensor created by integrating the maps produced by the previous layers. The GoogLeNet on the other hand, extracts deep features and widens the convolutional network to enhance training results. The model parameters are significantly reduced by two auxiliary classifiers, dimensionality reduction and mapping using a 1×1 convolutional kernel and the fully connected layer instead of the average pooling layer. The model was created to classify original image in the domain (\mathcal{D}_1). The dataset of labelled images is shown as

$$\mathcal{D}_1 = \{x_j, y_j\}_{j=1}^{10^6} \quad (5)$$

where $y_j \in \{1, \dots, 1000\}$ for class labels. The transfer learning concept can be applied to a deep CNN method to learn features of images in a different domain. This technique has adapted GoogLeNet to our application domain (\mathcal{D}_2), which is determined by the transfer learning methods. GoogLeNet transfer learning is the concept behind the suggested application.

$$\mathcal{D}_2 = \{x_j, y_j\}_{j=1}^{3064} \quad (6)$$

where the class labels, $y_j \in \{1, 2, 3\}$, represent the segmentation process. The system uses the pooling layer activations to represent the images' features. An image's feature vector, x_i is represented as

$$H(x_i) \in H^{1024} \quad (7)$$

The output of feature extracted functions are represented by H applied to input x_i . H^{1024} represents the output in vector with 1024 dimensions. The detection sequence is transformed into a feature vector when each pixel is extracted using DeGoNet.

3.4 Classification

Gated Self-Attentive Convolved MobileNetV3 (GSACMNet) is used to classify the ALD with minimal time complexity. Even as the number of images grows, the DL method minimizes training fluctuations and correctly diagnoses the infected. To improve accuracy in terms of speed and size, the MNetV3 approach is presented. MNetV3 uses depth-wise convolutions (DC) to improve training. The DC is one of the learnable parameters used to retrieve spatial information from each input channel during picture training. MNetV3 blocks and components are heavily influenced by the methods used in MNetV1 and MNetV2. As an alternative to the sigmoid function, the MNetV3 employs a non-linearity function known as hard-swish (h-swish).

$$h - swish(u) = u \times \sigma(u) \quad (8)$$

$$\sigma(u) = \frac{6(u+3) \times ReLU}{3} \quad (9)$$

The piece-wise linearity analog function is denoted by $\sigma(u)$ in this instance. The inverted residual (IR) block, which combines the DC and squeeze-excitation (SE) blocks, is a crucial component of the MNetV3 network approach. One type of bottleneck block that improves FMs with less

complexity is the IR block, which adds the input and output of related channels. The BN and h-swish functions are included in the DC separable, along with 1×1 point-wise kernels. By altering the convolution layers (CL), the DC separable increases the model's capability. During the training process, the SE block aids in concentrating just on pertinent characteristics.

The MNetV3 technique combines the gated convolution (GC) and dilated self-attentive (DSA) modules to efficiently acquire the key features. Here, we employ 3×3 CL and dual SA modules with 3×3 dilated convolution rates of $r = 2$ and $r = 3$. The GC then generates a deep distinguishable extraction process using the features from the DSA module with $r = 2$ and the 3×3 CL. The features from the 3×3 CL are combined and fed into the GC modules to create the final output. To extract global and local information, the encoder is subjected to Triple CL, which yield the mapped features x, y, and z, respectively. The characteristics x and y are then rewritten using the SoftMax layer to accomplish matrix multiplication.

$$A = \text{reformulate}(x)$$

$$B = \text{reformulate}(y)$$

$$C = \text{reformulate}(z)$$

$$P_{uv} = \frac{\exp(A_u B_v)}{\sum_{z=1}^m \exp(A_z B_v)} \quad (10)$$

$$DSA(P, Z) = P \times T \quad (11)$$

Here, P_{uv} indicates the effect of u^{th} and v^{th} locations, m indicates the total pixels, A, B and C indicates the reformulated features (RF). Also, P indicates the location of the attention maps and it is increased with RF C to obtain the final DSA outcome.

$$G = X_g \times I_{high} \quad (12)$$

$$I = X_l \times I_{low} \quad (13)$$

$$K = \varphi(I) \times \sigma(G) \quad (14)$$

In this instance, X_g and X_l represent the related matrices of two convolutional processes, while I_{high} and I_{low} represent the two inputs. G is the attention map, I is the embedded features, σ is the sigmoid function that falls between [0, 1], and φ is the ReLU function. However, the GSACMNet performance frequently declines as a result of significant regularization issues and lengthy training periods. In order to address this, efficient optimizers must adjust the network model parameters to minimize both the training complexity and the neurons random initialization.

4. RESULTS AND DISCUSSION

The APSE-NET is implemented using MATLAB (2020b) and operates on a server configured with an Intel Xeon F8 CPU running at 3.5 GHz, 64 GB of RAM and an NVIDIA GPU with an 11 GB graphics card.
















| Input image | Pre-processing | Feature extraction | Classification |
|---|---|--|--------------------|
|  |  |  | Normal |
|  |  |  | Apple scab |
|  |  |  | Powdery mildew |
|  |  |  | Frog eye leaf spot |
|  |  |  | Black rot |

Figure 3. Experimental result of the APSE-NET

Figure 3 demonstrates the simulation results of the APSE-NET utilizing different apple leaf image samples. Column 1 presents the leaf images and column 2 displays the pre-processed images. Column 3 illustrates the feature extraction images. Finally, Column 4 shows the classification output.

4.1 Performance analysis

The evaluation of the proposed APSE-NET model including AC, PR, SP, RE, MCC and F1 are utilized to determine the efficiency of the APSE-NET for detecting leukemia.

$$SP = \frac{T_{neg}}{T_{neg} + F_{pos}} \quad (15)$$

$$PR = \frac{T_{pos}}{T_{pos} + F_{pos}} \quad (16)$$

$$RE = \frac{T_{pos}}{T_{pos} + F_{neg}} \quad (17)$$

$$AC = \frac{T_{pos} + T_{neg}}{\text{Total no. of samples}} \quad (18)$$

$$F1 = 2 \left(\frac{\text{Precision} + \text{Recall}}{\text{Precision} + \text{Recall}} \right) \quad (19)$$

$$MCC = \frac{T_{pos} \times T_{neg} - F_{pos} \times F_{neg}}{\sqrt{(T_{pos} + F_{pos}) \times (T_{pos} + F_{neg}) \times (T_{neg} + F_{pos}) \times (T_{neg} + F_{neg})}} \quad (20)$$

Where T_{neg} and T_{pos} specifies true negatives and true positives of the sample images, F_{neg} and F_{pos} requires false negatives and false positives of the sample images

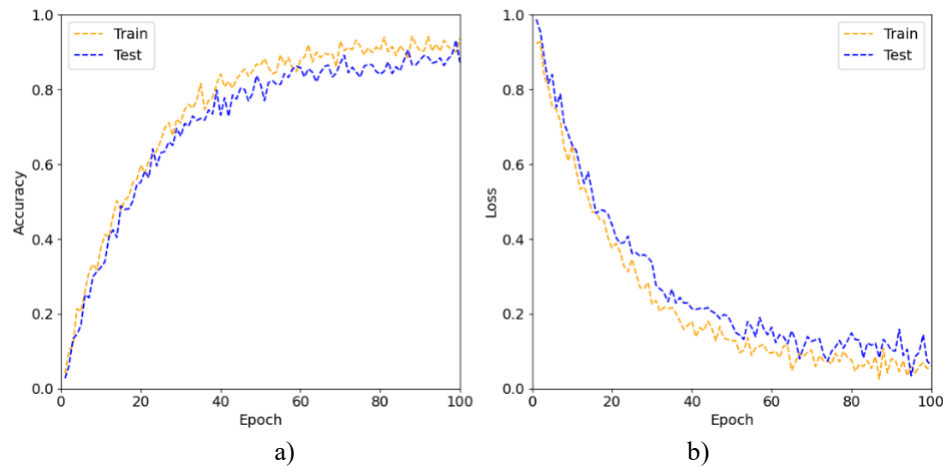


Figure 3. a) Accuracy and b) loss graph of the proposed APSE-NET

The accuracy and loss graph of the APSE-NET are displayed in Figure 3 a) and b). The performance of the APSE-NET is evaluated by the following parameters: AC, RE, F1, SP and PR. The accuracy curve is defined in Figure 3 a), where accuracy and epochs are positioned on opposite axes. The model's accuracy rises as the number of epochs grows. The epoch versus loss curve in Figure 4 b) displays that the model's loss reductions as the number of epochs increases. A 98.59% accuracy is accomplished by the APSE-NET.

4.2 Comparative analysis

In this section presents a contrast study of the APSE-NET in comparison of other DL models. To show results of

Table 1. Performance assessment of the APSE-NET

| Classes | AC | RE | PR | F1 | MCC |
|--------------------|-------|-------|-------|-------|-------|
| Normal | 97.56 | 96.13 | 98.21 | 91.85 | 91.43 |
| Apple scab | 98.89 | 96.40 | 96.71 | 95.90 | 94.89 |
| Powdery mildew | 98.96 | 97.14 | 97.54 | 93.62 | 96.10 |
| Frog eye leaf spot | 99.45 | 99.65 | 99.87 | 92.74 | 90.02 |
| Black rot | 98.10 | 98.61 | 93.72 | 95.04 | 92.54 |
| Overall | 98.89 | 97.58 | 97.21 | 94.76 | 95.49 |

Table 1 presents the performance metrics for detecting various types of APD using a classification system. The parameters include PR, F1, SP, AC, MCC and RE for each disease classes like normal, Apple scab, Powdery mildew, Frog eye leaf spot, Black rot. A total AC of 98.59% is attained by the APSE-NET using the gathered dataset. The proposed APSE-NET achieved 97.21%, 94.76%, 95.49% and 97.58% overall PR, F1, SP, MCC and RE identifying the dual kinds of leukemia based on the gathered dataset. Overall, the classifier demonstrates robust performance in distinguishing between different disease stages.

Table 2. Assessment of the proposed technique compared to existing techniques

| Networks | AC | PR | RE | F1 |
|------------|-------|-------|-------|-------|
| DenseNet | 95.75 | 95.43 | 90.13 | 85.38 |
| RegNet | 97.02 | 91.02 | 95.17 | 92.37 |
| ShuffleNet | 96.38 | 93.19 | 94.32 | 91.14 |

| | | | | |
|--------------------|-------|-------|-------|-------|
| MobileNet | 97.76 | 96.40 | 93.45 | 93.83 |
| GSACMNet (ours) | 98.89 | 97.21 | 97.58 | 94.76 |

Table 2 shows that the comparative analysis of APSE-NET method obtained 98.59% of AC, 97.21% of PR, 97.58% of RE and 94.76% of F1 respectively. The proposed GSACMNet technique improves the accuracy range of 3.31%, 1.95%, 2.63% and 1.18% better than DenseNet, RegNet, ShuffleNet and MobileNet respectively.

Table 3. Comparison of accuracy with existing and proposed work

| Author | Methods | Accuracy |
|--------------------------|----------|----------|
| Wang, Y., et al., [10] | CBAM | 94.0% |
| Hasan, S., et al., [11] | DWT | 98.63% |
| Bansal, P., et al., [14] | CNN | 96.25% |
| Proposed | APSE-NET | 98.89% |

Table 3 shows that proposed APSE-NET expands the overall accuracy of 4.88%, 0.26% and 2.74% better than CBAM, DWT and CNN. The comparison above indicates that in terms of precision, the proposed APSE-NET outperforms the current models.

5. CONCLUSION

This research proposed a novel APSE-NET for ALD detection. The input images are preprocessed by JBF to reduce the noise and enhance the image quality. The denoised images are fed into DeGoNet that combines the dense connectivity of DenseNet with the architectural principles of GoogleNet to efficiently capture multi-scale features. GSACMNet integrates self-attention and gating mechanisms into MobileNetV3, enabling it to focus on vital regions of the image. It effectively uses the extracted features for accurate and efficient classification. The proposed APSE-NET model achieves a high accuracy of 98.89% in ALD classification. The proposed GSACMNet technique improves the accuracy range of 3.31%, 1.95%, 2.63% and 1.18% better than DenseNet, RegNet, ShuffleNet and MobileNet respectively. Compared to CBAM, DWT and CNN the proposed model improves overall accuracy by 4.88%, 0.26% and 2.74% respectively. In future work, advanced transformer-based models can be explored to improve the detection of multiple co-occurring diseases on apple leaves under varying environmental conditions.

CONFLICTS OF INTEREST

The authors declare that there is no conflict of interest.

FUNDING STATEMENT

Not applicable.

ACKNOWLEDGEMENTS

The author would like to express his heartfelt gratitude to the supervisor for his guidance and unwavering support during this research for his guidance and support.

REFERENCES

- [1] Z.A. Shah, M.A. Dar, E.A. Dar, C.A. Obianefo, A.H. Bhat, M.T. Ali, M. El-Sharnouby, M. Shukry, H. Kesba, and S. Sayed, "Sustainable fruit growing: An analysis of differences in apple productivity in the Indian state of Jammu and Kashmir". *Sustainability*, vol. 14, no. 21, pp. 14544, 2022. [[CrossRef](#)] [[Google Scholar](#)] [[Publisher Link](#)]
- [2] O. Zhandybayev, A. Malimbayeva, and R. Zhumabayeva, Review of Modern Methods for Optimizing Apple Mineral Nutrition to Increase Yield and Fruit Preservation. *Почвоведение и агрохимия*, vol. 2, pp. 78-93, 2024. [[CrossRef](#)] [[Google Scholar](#)] [[Publisher Link](#)]
- [3] N.I.K.I.T.A. Chauhan. Studies on arthropod pests of apple and their natural enemies in different farming systems (Doctoral dissertation, Ph. D. Thesis. Dr. Yashwant Singh Parmar University of Horticulture and Forestry, Nauni, Solan, HP. 383, 2024[[CrossRef](#)] [[Google Scholar](#)] [[Publisher Link](#)]
- [4] S.H. Alemu, "Apple cultivation as pathway out of poverty in highland Ethiopia: Value generation and income distribution at farm", *village and household level*. SI: sn, 2020[[CrossRef](#)] [[Google Scholar](#)] [[Publisher Link](#)]
- [5] S.U. Nabi, S. Parveen, W.H. Raja, I.M. Javid, S. Yasmin, M.A. Sheikh, and O.C. Sharma. "Diseases of apple (*Malus domestica*) and their management". *Agrica*, vol. 11, no. 1, pp. 32-40, 2022. [[CrossRef](#)] [[Google Scholar](#)] [[Publisher Link](#)]
- [6] B. Pokhrel, "Effects of environmental factors on crop diseases". *J Plant Pathol Microbiol*, vol. 12, no. 5, pp. 553, 2021. [[CrossRef](#)] [[Google Scholar](#)] [[Publisher Link](#)]
- [7] B. Chen, P. Yu, W.N. Chan, F. Xie, Y. Zhang, L. Liang, K.T. Leung, K.W. Lo, J. Yu, G.M. Tse, and W. Kang. "Cellular zinc metabolism and zinc signaling: from biological functions to diseases and therapeutic targets". *Signal transduction and targeted therapy*, vol. 9, no. 1, pp. 6, 2024. [[CrossRef](#)] [[Google Scholar](#)] [[Publisher Link](#)]
- [8] A.I. Khan, S.M.K. Quadri, S. Banday, and J.L. Shah, "Deep diagnosis: A real-time apple leaf disease detection system based on deep learning." *computers and Electronics in Agriculture*, vol. 198, pp. 107093, 2022. [[CrossRef](#)] [[Google Scholar](#)] [[Publisher Link](#)]
- [9] A.I. Khan, S.M.K. Quadri, S. Banday, and J.L. Shah, "Deep diagnosis: A real-time apple leaf disease detection system based on deep learning". *computers and Electronics in Agriculture*, vol. 198, pp. 107093, 2022. [[CrossRef](#)] [[Google Scholar](#)] [[Publisher Link](#)]
- [10] Y. Wang, Y. Wang, and J. Zhao. "MGA-YOLO: A lightweight one-stage network for apple leaf disease detection". *Frontiers in plant science*, vol. 13, pp. 927424, 2022. [[CrossRef](#)] [[Google Scholar](#)] [[Publisher Link](#)]
- [11] S. Hasan, S. Jahan, and M.I. Islam, "Disease detection of apple leaf with combination of color segmentation and modified DWT". *Journal of King Saud University-Computer and Information Sciences*, vol. 34, no. 9, pp. 7212-7224, 2022. [[CrossRef](#)] [[Google Scholar](#)] [[Publisher Link](#)]
- [12] X. Gong, and S. Zhang. "A high-precision detection method of apple leaf diseases using improved faster R-CNN". *Agriculture*, vol. 13, no. 2, pp. 240, 2023. [[CrossRef](#)] [[Google Scholar](#)] [[Publisher Link](#)]

- [13] J. Di, and Q. Li, A method of detecting apple leaf diseases based on improved convolutional neural network. Plos one, vol. 17, no. 2, p.e 0262629, 2022. [[CrossRef](#)] [[Google Scholar](#)] [[Publisher Link](#)]
- [14] P. Bansal, R. Kumar, and S. Kumar, "Disease detection in apple leaves using deep convolutional neural network". *Agriculture*, vol. 11, no. 7, pp. 617, 2021. [[CrossRef](#)] [[Google Scholar](#)] [[Publisher Link](#)]
- [15] X. Huang, D. Xu, Y. Chen, Q. Zhang, P. Feng, Y. Ma, Q. Dong, and F. Yu. "EConv-ViT: A strongly generalized apple leaf disease classification model based on the fusion of ConvNeXt and Transformer". *Information Processing in Agriculture*, 2025 [[CrossRef](#)] [[Google Scholar](#)] [[Publisher Link](#)]
- [16] W. Bao, and F. Zhang, "Apple Pest and Disease Detection Network with Partial Multi-Scale Feature Extraction and Efficient Hierarchical Feature Fusion", *Agronomy*, vol. 15, no. 5, pp. 1043, 2025 [[CrossRef](#)] [[Google Scholar](#)] [[Publisher Link](#)]

AUTHORS



Sarika Tanajirao Thorat is a research scholar in Electronics and Communication Engineering Department, JJTU, Rajasthan, India and working as an Assistant Professor at Nutan Maharashtra Institute of Engineering and Technology, Talegaon Dabhade, Pune, Maharashtra, India. She has completed her M.Tech. (Electronics-VLSI) from Bharati Vidyapeeth University, Pune, Maharashtra, India. Ms. Sarika has 18 years of Teaching and 2 years Industry

experience. She has published 10 articles in National and International Conferences and journals. She has 3 patents (National), 2 copyrights. She is Life member of ISTE and IAENG. Her research interest areas are Embedded System, IOT, Machine Learning.



Rahul Kumar Budania is an accomplished educator with a strong academic background and a wealth of professional experience. Currently serving as an Assistant Professor and Head of the Electronics & Communication Engineering department at Shri Jagdishprasad Jhabarmal Tibrewala University, Jhunjhunu, Rajasthan, India. Dr. Budania is dedicated to fostering knowledge and contributing to organizational success. Academically, Dr. Budania holds a Ph.D. in

Electronics and Communication Engineering from Shri Jagdishprasad Jhabarmal Tibrewala University. His M. Tech in ECE was completed at Pratap University, Jaipur, India. His journey began with a B. Tech in ECE from Arya Institute of Engineering & Technology, Jaipur, in 2014. Dr. Budania's scholarly contributions are showcased in his publications. Notably, he has National & International patents and authored various research papers published SCOPUS Journals like mathematical statistician and engineering applications, international journal of mobility technology by ARAI, Journal of Mines, Metal and Fuels etc. His dedication to the field is further exemplified by his IAENG (International Association of Engineers) membership, signifying his involvement in the global engineering community.

Arrived: 05.07.2025

Accepted: 12.08.2025